INL/CON-07-12676
PREPRINT

3D CFD Model of a Tubular Porous-Metal Supported Solid Oxide Electrolysis Cell

2007 Fuel Cell Seminar

G. Hawkes
B. Hawkes
M. Sohal
P. Torgerson
T. Armstrong
M. Williams

October 2007

The INL is a
U.S. Department of Energy
National Laboratory
operated by
Battelle Energy Alliance

This is a preprint of a paper intended for publication in a journal or proceedings. Since changes may be made before publication, this preprint should not be cited or reproduced without permission of the author. This document was prepared as an account of work sponsored by an agency of the United States Government. Neither the United States Government nor any agency thereof, or any of their employees, makes any warranty, expressed or implied, or assumes any legal liability or responsibility for any third party's use, or the results of such use, of any information, apparatus, product or process disclosed in this report, or represents that its use by such third party would not infringe privately owned rights. The views expressed in this paper are not necessarily those of the United States Government or the sponsoring agency.

3D CFD Model of a Tubular Porous-Metal Supported Solid Oxide Electrolysis Cell

G. Hawkes[1], B. Hawkes[1], M. Sohal[1], P. Torgerson[2], T. Armstrong[3], M. Williams[2]

[1]Idaho National Laboratory, Idaho Falls, Idaho

[2]Worldwide Energy Inc., Butte, Montana

[3]Oak Ridge National Laboratory, Oak Ridge, TN

Currently there is strong interest in the large-scale production of hydrogen as an energy carrier for the non-electrical market [1, 2, and 3]. High-temperature nuclear reactors have the potential for substantially increasing the efficiency of hydrogen production from water splitting, with no consumption of fossil fuels, no production of greenhouse gases, and no other forms of air pollution. A high-temperature advanced nuclear reactor coupled with a high-efficiency high-temperature electrolyzer could achieve a competitive thermal-to-hydrogen conversion efficiency of 45 to 55%. A research program is under way at the INL to simultaneously address the research and scale-up issues associated with the implementation of solid-oxide electrolysis cell technology for hydrogen production from steam. The future SOEC market includes the 1200MW GEN4 reactor which has projected 40-50% efficiency, 400 tones H2 production per day (at 5kg H2/car/300 mile day this corresponds to 80,000 cars/day). DOE is planning for 26GW of nuclear hydrogen production by 2025.

Worldwide Energy, Inc. (WE) is the only corporation solely pursuing metal supported tubular design. The SOFC and SOEC development are in parallel with the intention to develop a reversible SOFC. Standard materials for YSZ electrolyte, Ni-YSZ anode, and standard materials for cathode - LSM, LSF, and LSCF - are being considered initially. Of course, development and optimization of different materials may be necessary and stack designs could be different since a larger cathode chamber is necessary for the SOFC. What is extremely interesting about the porous metal-supported technology is that all the ceramic components are inside the tube and because of the relative coefficients of thermal expansion (CTE's), they are expected to be compression. The ceramic CTE's are closely matched to YSZ, but the porous tube should be greater if not matched to YSZ, resulting in compression of the ceramic layers.

It is essential to understand the fundamental electrochemical performance of the SOEC. Figure 1 shows the basic thermodynamic data, the Gibbs free energy of reaction, $\Delta^R G$ (T), $T\Delta^R S$ (T), enthalpy of reaction, $\Delta^R H$ (T), for the electrolysis of water using the MALT2 thermodynamic database. These are positive values whereas for the oxidation of hydrogen, the reverse reaction, they are negative values, kilojoule per mole.
In general $\Delta^R G$ (T) is calculated from the heat capacities (Cp) of the species involved as a function of T and from values of both enthalpy and entropy at a reference temperature, usually 298K. However, MALT2 provides all thermodynamic values at any temperature. Specifically for this paper,
H2 + 1/2 O2 = H2O (fuel cell)
H2O = H2 + 1/2 O2 (electrolyser steam hydrolysis)

For the steam hydrolysis reaction $\Delta^R H$ is the total energy provided. The reaction is endothermic. As the temperature is increased, less electrical energy is required. If waste heat from geothermal or nuclear power plants is available, the steam generation or pre-heating costs and $T\Delta^R S$ thermal energy requirements could be provided in a cost effective manner. This is why the nuclear industry is, of course, interested in the electrolyser technology. The higher temperature also improves reaction kinetics. During isothermal electrolysis, the current is increased moving from the OCV. Outside heat must be added to provide the $T\Delta^R S$ term. Electrical energy provides $\Delta^R G$ and I^2R term provides some of the heat but not all

From the First Law:
Equation (1)

$$Q + W = -\dot{N}_{H2}\,\Delta^R H$$

Letting $Q = 0$ (no external heat transfer), $W = VI$ (where W is the electrical work) and noting that the electrical current is directly related to the molar production rate of hydrogen by:
Equation (2)

$$\dot{N}_{H2} = I/2F$$

where F is the Faraday number (F = 96,487 J/V mol), yields
Equation (3)

$$V_{tn} = \frac{-\Delta^R H}{2F}$$

In the adiabatic operation mode, no heat is added but the temperature of the electrolyser and its flow inlet and outlet streams is reduced as heat is supplied. At V_{tn}, the thermal neutral voltage, no Q heat is provided and the I^2R tem provides all the thermal energy. $\Delta^R G$ for the electrochemical reaction is provided. V_{tn} is obviously a good point to operate an electrolyser. Above the V_{tn}, the electrolyser must begin to reject heat. This paper uses the Wark [4] sign conventions: Q in – positive; Q out – negative; Work in – positive; Work out – negative; $\Delta H_{formation} = \Delta^R H$ - negative for exothermic reaction; fuel cell I – positive; fuel cell Voltage negative; SOEC, I – negative; SOEC Voltage negative. From the definition of electrical work, one can define the reversible voltage,
Equation (4)

$$E_R(T) = \frac{\Delta^R G(T)}{2F}$$

E_R (T) for a given temperature is the 'reversible voltage or potential'. $\Delta^R G°$ (T) is the standard state Gibbs free energy change for a reaction at the standard state pressure (1 atm - 1 bar) and at temperature T. E° (T) is the standard reversible voltage (at 1 atm) given by:
Equation (5),

$$E^o(T) = \frac{\Delta^R G^o(T)}{2F}$$

Since the Gibbs free energy change for a reaction is the sum of the standard state Gibbs free energy change for a reaction at the standard state pressure and the equilibrium product Kp or
Equation (9),

$$\Delta G^R(T) = \Delta^R G^o(T) + RT \ln(Kp)$$

the E_R (T) can be expressed as a form of the Nernst equation which is:
Equation (10)

$$E_R(T) = E^o - \frac{RT}{nF}\ln\left[\left(\frac{y_{H2O}}{y_{H2}\,y_{O2}^{1/2}}\right)P^{-1/2}\right]$$

where P is the pressure, n the number of electrons transferred, and the yi are the molar fractions (Pi = yi P).
E^o for the electrolyser decreases with increasing temperature while V_{tn} increases with increasing temperature. The lower the V_{tn}, the lower the temperature of operation, and the sooner (lower operating voltage) that the electrolyser must start removing heat. The closer the V_{tn} and E^o lines are together the sooner the electrolyser must begin rejecting heat. The following equations are the conventional definitions [5, 6] of basic thermal efficiency and the relationships among thermal and

exergetic efficiency as well as the other primary electrolyser variables. For thermal efficiency one has:

Equation (11)

$$\eta_t = \frac{\Delta^R H \dot{N}_{H2}}{VI}$$

Simplifying Equation (11) using Equation (2), one obtains

Equation (12)

$$\eta_t = \frac{\Delta^R H / 2F}{V}$$

Simplifying Equation (12) using Equation (3), one obtains

Equation (13)

$$\eta_t = \frac{V_{tn}}{V}$$

The expression for the maximum thermal efficiency for an electrolyser is:

Equation (14)

$$\eta_{t,Max} = \frac{\Delta^R H}{\Delta^R G}$$

Exergetic efficiency is defined as maximum work divided by the actual work,

Equation (15)

$$\zeta = E_R(T)/V$$

or

Equation (16)

$$\eta_t = \frac{\Delta^R H / 2F}{V} = \frac{V_{tn}}{V} = \zeta \eta_{t,Max}$$

Electrolysis thermal efficiency is strictly speaking is the heating value H2 divided by the power and heat input. Steam penalty (heat required to heat up steam is not taken into account) in the standard efficiency definition. The system efficiency must account for thermal to H2. It is very interesting to note that maximum thermal efficiency (Equation 5) equals the thermal efficiency times the exergetic efficiency (zeta) or that the exergetic efficiency (E_R/V) is the simple multiplier between actual and theoretical thermal efficiency. Maximum electrolyser efficiency occurs at E^o, but there the current is zero and operation impractical. From Figure 2 one can see electrolyser maximum thermal efficiency increases with increasing temperature. The lower the temperature of operation, the lower the electrolyser theoretical efficiency. This is based on thermodynamic analysis alone. The lower the OCV (higher temperature), the higher the theoretical efficiency. At theoretical efficiency V=OCV.

Several detailed models, which take into account gas transport through porous electrodes, electrochemical reactions at the electrodes (near electrode/electrolyte interfaces), and ohmic losses have been developed. The vast majority of them, however, are numerical due to the analytical complexities involved. Also, quantitative validation of virtually these models is generally difficult for lack of experimentally verifiable/measurable parameters used in many of the models. Nonetheless, INL has considerable experience with the Fluent model [7-11]. The other authors also

have considerable reversible fuel cell and electrolyser familiarity [12-15]. Many details are presented elsewhere on the details of the modeling [16, 17]. Many model parameters were known from experimental data, button cell tests, literature values, or values from previous electrolyzer test and simulations. Flow is co-current. The current collector on the O2 side is a straight wire - this is not actually what is used. It is in intimate contact with the O2 electrode for this model. The finite element is taken axial down the entire length of the tube. The operating Pressure is 101,000 Pa. The activation overpotentials for both electrodes were for this first simulation assumed to be zero. Material properties based on button cell tests from MTSOFC and anode-supported design test at ORNL which have 2.0 w/cm2 using LSM cathode in SOFC-mode. All calculations were conducted for SOEC adiabatic operation at 800°C. Shown in Figure 3 is the tube schematic. In Figure 4 are shown the current densities in the electrolyte (all contour plots are for 7.0 Amps). Note that the current for all contour plots is 7.0 Amps which corresponds to an average of around 0.3 amp/cm^2. Units in Figure 4 are shown in Amps/m^2. Current density is greatest magnitude at blue area. Blue occurs because all current in tube has to be gathered at very end. There is not as much current density going into the current collector in the middle because there aren't any end effects from the current spreading out and gathering in. Unexpectedly, most of the electrolysis work is being done at the high current and high voltage end. The Nernst voltage is calculated from concentrations at the electrolyte interfaces. Current density depends on Nernst voltage. Nernst voltage depends on temperature and concentrations. Temperature depends on current density. This is why the temperature is high - from the I^2R term.

In the present work a 3D CFD model has been created to model high-temperature steam electrolysis in the new novel porous metal tubular SOEC. This may be the first reported modeling effort on this type of SOEC. Results to-date provide detailed profiles of temperature, Nernst potential, operating potential, hydrogen-side gas composition, oxygen-side gas composition, current density and hydrogen production over a range of stack operating conditions.

REFERENCES

1) International Atomic Energy Agency (IAEA), May 1999, *Hydrogen as an energy carrier and its production by nuclear power*, IAEA-TECDOC-1085.
2) National Academy of Sciences, National Research Council, *The Hydrogen Economy: Opportunities Costs, Barriers, and R&D Needs*, February, 2004.
3) Yildiz, B., and Kazimi, M. S., "Nuclear Energy Options for Hydrogen and Hydrogen-Based Liquid Fuels Production," MIT-NES-TR-001, September 2003.
4) Wark, Kenneth, "Thermodynamics", 3rd Edition, McGraw-Hill, 1977.
5) EG&G Technical Services, Science Applications International Corporation, *Fuel Cell Handbook*, 6th Edition, Editor M.C. Williams, DOE/NETL 2002/1179, 2002.
6) Hoogers, G. (ed.), *Fuel Cell Technology Handbook,* CRC Press, New York, 2003.
7) Herring, J. S., O'Brien, J. E., Stoots, C. M., Lessing, P. A., Anderson, R. P., Hartvigsen, J. J., and Elangovan, S., "Hydrogen Production from Nuclear Energy via High-Temperature Electrolysis," presented at the 2004 International Conference on Advances in Nuclear Power Plants (ICAPP '04), June 13-17, 2004, Pittsburgh, PA.
8) Herring, J. S., O'Brien, J. E., Stoots, C. M., Lessing, P. A., Anderson, R. P., Hartvigsen, J. J., and Elangovan, S., "Hydrogen Production through High-Temperature Electrolysis Using Nuclear Power," presented at the AIChE Spring National Meeting, New Orleans, April 25 – 29, 2004.
9) O'Brien, J. E., Stoots, C. M., Herring, J. S., and Lessing, P. A., "Characterization of Solid-Oxide Electrolysis Cells for Hydrogen Production via High-Temperature Steam Electrolysis,"Proceedings, 2nd International Conference on Fuel Cell Science, Engineering, and Technology, June 14-16, 2004, Rochester, NY, paper# 2474, pp., 219 – 228.
10) O'Brien, J. E., Stoots, C. M., Herring, J. S., and Lessing, P. A., "Performance Measurements of Solid-Oxide Electrolysis Cells for Hydrogen Production from Nuclear Energy," Proceedings, 12thICONE Meeting, April 25-29, 2004, Arlington, VA, paper # ICONE12-49479.
11) O'Brien, J. E., Stoots, C. M., Herring, J. S., and Hartvigsen, J. J., "High-Temperature Electrolysis for Hydrogen Production from Nuclear Energy," NURETH-11 Conference, October 2-6, 2005, Avignon, France.

12) Williams, M.C., "Electrode Performance in Reversible SOFC's," with Olga Marina and Larry Pederson, *J. Journal of The Electrochemical Society*, 154, (5), B452-B459 (2007).
13) Williams, M.C., "Reversible SOFC Development," with K. R. Sridhar, in *Proceedings of the Ninth International Symposium on Solid Oxide Fuel Cells (SOFC-IX)*, Vol. 1 Cells, Stacks and Systems, Editor S.C. Singhal and J. Mizusaki, pp. 20-31, Quebec City Convention Center, Quebec City, Canada, May 15-20, 2005.
14) Williams, M.C., "Hydrogen Economy Based on Renewable Energy Sources," with John A. Turner and Krishnan Rajeshwar, *Interface*, **13**, No. 3, pp. 24-30, (2004).
15) Williams, M.C., "Hydrogen Production from Fossil Fuels with High Temperature Ion Conducting Ceramics," with Eric D. Wachsman, *Interface*, **13,** No. 3, pp. 32-27, (2004).
16) Prinkey, M., Shahnam, M., and Rogers, W. A., "SOFC FLUENT Model Theory Guide and User Manual," Release Version 1.0, FLUENT, Inc., 2004.
17) FLUENT Theory Manual, version 6.1.22, Fluent Inc., Lebanon, New Hampshire, 2004.

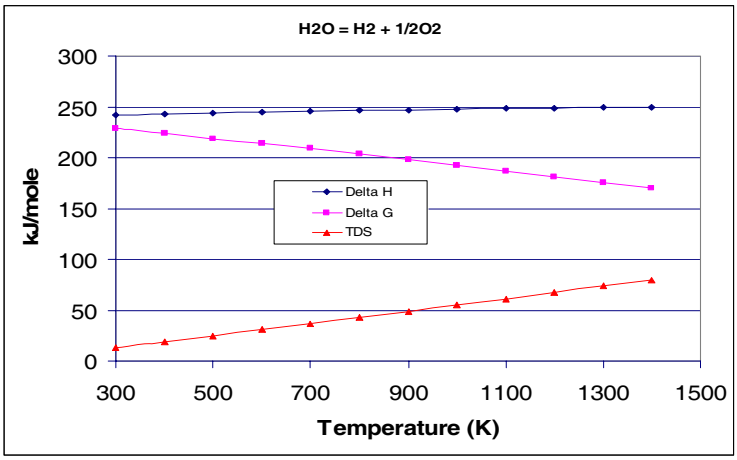

Figure 1. Efficiency advantage of high temperature electrolysis.

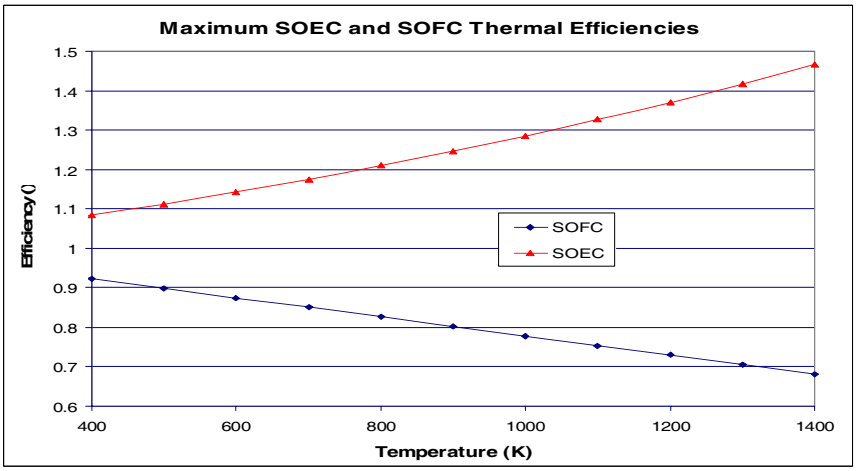

Figure 2. Maximum SOEC and SOFC thermal efficiencies.

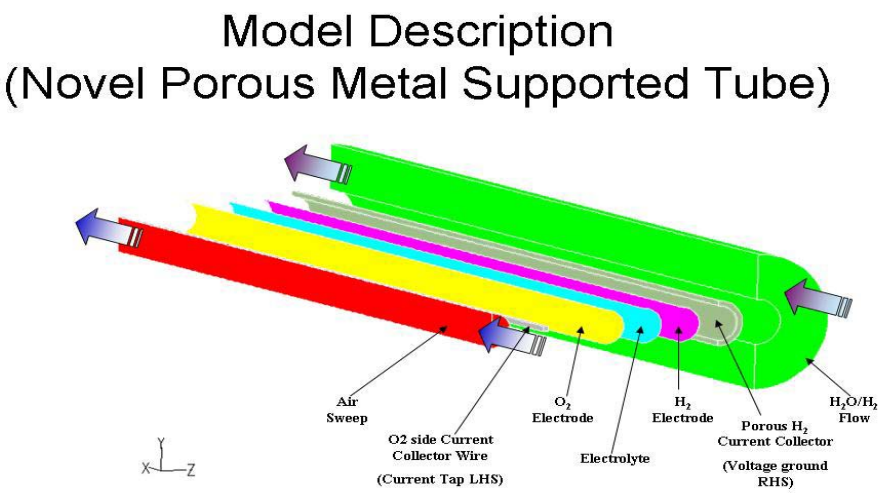

Figure 3. WE MTSOFC cut-away section.

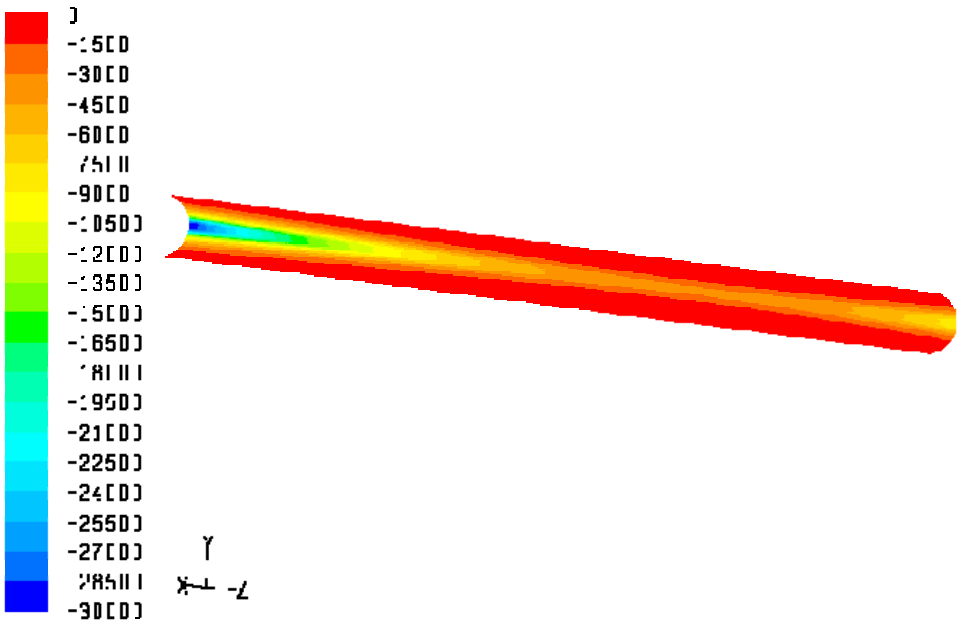

Figure 4. Current density in electrolyte (all contour plots are for 7.0 Amps, units are Amps/m^2).